THE JOURNAL OF PHYSICAL CHEMISTRY B

Article

pubs.acs.org/JPCB

Hydrated Excess Protons Can Create Their Own Water Wires

Yuxing Peng,[†] Jessica M. J. Swanson,[†] Seung-gu Kang,[‡] Ruhong Zhou,[‡] and Gregory A. Voth*,[†]

[†]Department of Chemistry, James Franck Institute, Computation Institute, The University of Chicago, 5735 South Ellis Avenue, Chicago, Illinois 60637, United States

[‡]Computational Biology Center, IBM Thomas J. Watson Research Center, Yorktown Heights, New York 10598, United States

ABSTRACT: Grotthuss shuttling of an excess proton charge defect through hydrogen bonded water networks has long been the focus of theoretical and experimental studies. In this work we show that there is a related process in which water molecules move ("shuttle") through a hydrated excess proton charge defect in order to wet the path ahead for subsequent proton charge migration. This process is illustrated through reactive molecular dynamics simulations of proton transport through a hydrophobic nanotube, which penetrates through a hydrophobic region. Surprisingly, before the proton enters the nanotube, it starts "shooting" water molecules into the otherwise dry space via Grotthuss shuttling, effectively creating its own water wire where none existed before. As the proton enters the nanotube (by 2−3 Å), it completes the solvation process, transitioning the nanotube to the fully wet state. By contrast, other monatomic cations (e.g., K^+) have just the opposite effect, by blocking the wetting process and making the nanotube even drier. As the dry nanotube gradually becomes wet when the proton charge defect enters it, the free energy barrier of proton permeation through the tube via Grotthuss shuttling drops significantly. This finding suggests that an important wetting mechanism may influence proton translocation in biological systems, i.e., one in which protons "create" their own water structures (water "wires") in hydrophobic spaces (e.g., protein pores) before migrating through them. An existing water wire, e.g., one seen in an X-ray crystal structure or MD simulations without an explicit excess proton, is therefore not a requirement for protons to transport through hydrophobic spaces.

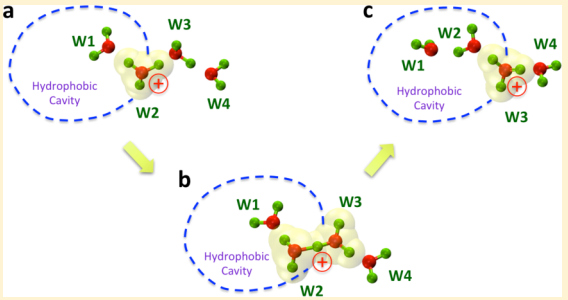

INTRODUCTION

The process of hydrated excess proton solvation and transport in aqueous systems displays many unique characteristics due the unique nature of the net positive charge defect that an excess proton creates.[1−5] By altering the covalent bonds and hydrogen bonds of surrounding solvent molecules, the hydrated excess proton charge defect is strongly delocalized and creates a series of dynamically interchanging structures (i.e., the Zundel $H_5O_2^+$ and Eigen $H_9O_4^+$ cations).[2,6,7] Because of this charge defect delocalization, the hydrated excess "proton" (or more accurately stated, the charge defect) is also able to hop between neighboring water molecules by "structural diffusion" via successive hopping events involving the rearrangement of the local bonding topologies. This shuttling process, known as the "Grotthuss mechanism",[1−4,6−13] is crucial to a number of fundamental processes in chemistry, physics, biology, and materials science.

In biology, protons are widely used for the transduction of signals and energy (e.g, in channels, transporters, and enzymes). They are transported through both protonatable residues and buried water molecules via Grotthuss shuttling.[3,4,11] Hence, studies on proton transport (PT) in biological systems have almost always started with the assumption that PT follows aqueous (already hydrated) pathways, which can be obtained from experimental data or by computational predictions.[14−16] However, hydrophobic regions are commonly found in proteins,[17−20] which complicates the interpretation of PT.

Carbon nanotubes (CNTs) have provided insight into the solvation and ion transport properties of homogeneous hydrophobic spaces. Experiments and computer simulations have shown that water molecules can stably occupy the interior of CNTs.[21−23] Theoretical studies[24−29] and recent experiments[30] have further shown that proton diffusion through nanoconfined spaces, such as hydrophobic channels and nanotubes, can be facile (and possibly even faster than in bulk water). These results provide support for the supposition that the hydrophobic spaces in biomolecules may also transiently contain water molecules capable of proton conduction. However, a common assumption is that hydrophobic spaces must be solvated *prior* to PT. This logic has led to numerous mechanistic predictions based on the existence of a quasi-stable water wires (e.g., see refs 31−33). However, it has also been clearly demonstrated that the presence of an excess proton greatly influences the local water solvation structure (see ref 4 for a discussion). In the present work, it is in fact found that as soon as a charge defect associated with a

Special Issue: Branka M. Ladanyi Festschrift

Received: September 19, 2014
Revised: November 1, 2014
Published: November 4, 2014

   dx.doi.org/10.1021/jp5095118 | J. Phys. Chem. B 2015, 119, 9212−9218

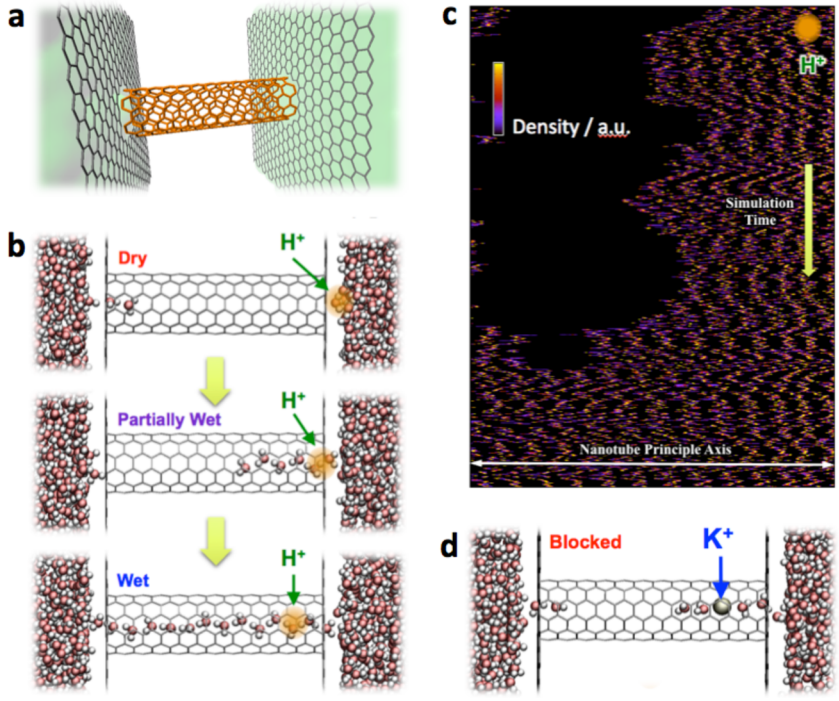

Figure 1. Simulations of ion transport through an originally "dry" nanotube as described in the text. (a) Construct of the simulation system. The armchair-type (6,6) CNT structure is assembled between two graphene single layers that separate the bulk water. (b) Overview of the proton induced wetting process along with the motion of the excess proton from bulk−tube interface into about 4 Å of the nanotube. (c) Real-time densities traces of the channel water molecules starting from a partially dry nanotube with the existence of the excess proton. Each bright line can represent the trace of the oxygen atom in a water molecule. (d) Simulation with the K^+ inside the nanotube, which remains mostly dry.

hydrated excess proton charge nears a hydrophobic space, the associated solvating water can experience a strong driving force *to fill that space*. Moreover, this finding naturally leads to the possibility that when an excess proton deprotonates from a peripheral amino acid residue or is solvated outside a hydrophilic (or amphiphilic) region, it can initiate additional solvation of such a region, which will in turn be coupled to the PT process through it.

Herein, multiscale reactive molecular dynamics (MS-RMD) is used to study PT through a CNT penetrating a graphene sheet. As described in the previous paragraph, a surprising phenomenon is revealed in which an excess proton charge defect creates its own aqueous transport pathway by shuttling water molecules *through it* into the hydrophobic nanoconfined space. This process can be described as a variant of Grotthuss shuttling, wherein water molecules travel *through* a hydrated excess proton charge defect. The induced wetting is shown to be excess proton specific; it does not happen when the excess proton (H^+) is replaced by K^+ or even a "classical" H_3O^+ (non-Grotthuss shuttling) cation model. The two-dimensional free energy surface reveals a three-step mechanism by which the protonic charge defect is transiently stabilized at the nanotube entrance, facilitates nanotube wetting via Grotthuss-facilitated water migration through the charge defect, and then traverses a lower free energy barrier for Grotthuss shuttling proton permeation via activated (infrequent event) dynamics. This finding has widespread implications for PT through hydrophobic (and likely other) regions in molecular systems such as proteins, by demonstrating that protons can dynamically create their own solvation pathways that would not be detected by experimental or computational means in absence of an *explicit* protonic charge defect.

METHODS

The system studied in this work consists of a 29.4 Å (*Z*-dimension) armchair-type (6,6) single walled carbon nanotube (CNT) with a single layer of graphene and bulk water on either side (Figure 1a). The space between the graphene layers was left empty (it is merely intended to provide a low dielectric environment). The graphene layers extend 41.82 and 42.5 Å in the *X* and *Y* dimensions and are replicated under periodic boundary conditions. The two slabs of water molecules on either side of the graphene sheets contain seven pairs of K^+ and Cl^- ions collectively. This type of (6,6) CNT has been the focus of previous computational work,[24,26,27,34−37] partially because its 8 Å diameter accommodates a single-file chain of water molecules, which is similar to the solvation structure found in some biological channels. As previously reported,[26] the use of standard force field parameters enables spontaneous wetting of a CNT of this diameter. Thus, to mimic hydrophobic environments, the LJ ε_{LJ} parameter for the CNT carbon atoms was reduced to provide a mostly dry (hydrophobic) CNT in unbiased molecular dynamics simulations, with only two to four water molecules transiently entering the mouth regions (Figure 1a).

The hydrated excess proton was treated explicitly with the multiscale reactive molecular dynamics (MS-RMD) method developed by the Voth group.[2,4,13,38−44] The multistate empirical valence bond version 3 (MS-EVB3) model[41] and the SPC/Fw[45] water model were used. All other parameters (for ions and carbon atoms) were taken from the standard CHARMM22 force field.[46] The depth of the Lennard-Jones potential well for CNT carbon atoms is scaled to 80% of the standard value to make the CNT more hydrophobic as noted above and hence dry in the absence of ions restrained to be in

dx.doi.org/10.1021/jp5095118 | J. Phys. Chem. B 2015, 119, 9212−9218

the CNT. The simulations were run with RAPTOR,[47] an in-house extension of the LAMMPS software.[48] The particle−particle, particle−mesh method[49] was used to treat long-range electrostatics. The Nosé−Hoover thermostat at 300 K and a time step of 1.0 fs were used.

To construct the free energy surface for the wetting process inside the CNT, we defined a water occupancy collective variable:

$$N_w = \sum_i^{N_{H_2O}} N_i \tag{1}$$

where N_{H_2O} is total number of the water molecules and N_i is the occupancy of the ith water molecule in a defined rectangular box:

$$N_i = \prod_\alpha^{x,y,z} \left(\frac{1 - R_{i,\alpha}^{\ 6}}{1 - R_{i,\alpha}^{\ 12}} \right) \tag{2}$$

The dimensionless coordinate $R_{i,\alpha}$ is defined as

$$R_{i,\alpha} = \begin{cases} 0 & (|r_{i,\alpha} - r_{0,\alpha}| \le b_\alpha) \\ \dfrac{|r_{i,\alpha} - r_{0,\alpha}| - b_\alpha}{d} & (|r_{i,\alpha} - r_{0,\alpha}| > b_\alpha) \end{cases} \tag{3}$$

where r_0 and r_i are the positions of the center of the CNT and the oxygen atom of the ith water molecule, respectively. A box similar to the shape of the CNT was defined by $b_x = b_y = 4.0$ Å and $b_x = 14$ Å, while d was chosen to be 5.0 Å to allow a smooth transition of the water occupancy from zero (when the molecule is at the graphene−water interface) to 1 (when the molecule is inside the CNT). The umbrella-sampling technique and the WHAM method[50] were used with the bias potential defined by

$$U_{bias}(z^+, N_w) = \frac{1}{2} k_z (z^+ - z_0)^2 + \frac{1}{2} k_{N_w} (N_w - N_0)^2 \tag{4}$$

applied to two independent "reaction coordinates": the Z-axis position of the positive charge (H^+, K^+, or H_3O^+) and the water occupancy number in the CNT. The resulting 2D free energy surface was constructed from 325 sampling windows covering the range of charge locations from 9.0 to 21.0 Å in 1.0 Å intervals and for water occupancies ranging from 2 to 14 with an interval of 0.5. The bias force constants were chosen to be 10.0 kcal mol^{-1} Å^{-2} and 5.0 kcal mol^{-1}, respectively, to ensure sufficient window overlap.

RESULTS AND DISCUSSION

Proton Induced Wetting of Hydrophobic Spaces. As described in the section Methods, the CNT studied herein was modified to be more hydrophobic and hence mostly dry. In unbiased MD simulations only one to two water molecules transiently enter the mouth regions on either side of the CNT (Figure 1a). These waters are partially stabilized by interactions with the graphene atoms, which were simulated with the standard LJ parameters. The hydrated excess proton (or more accurate the net positive charge defect associated with an excess proton) was described with the MS-RMD method, which as noted earlier has been shown to successfully model PT in numerous aqueous and biomolecular systems.[4,13,40,41,51] Since there is a large free energy penalty for any ion to shed its solvation shell and enter a nanoconfined hydrophobic region, umbrella sampling was used to calculate the free energy profiles for ion transport through the CNT as described in Methods.

Figure 1 shows how the charge defect associated with the hydrated excess proton strongly influences the CNT hydration. We note that hereafter this net positive charge defect will be referred to as just the "hydrated excess proton" or "the proton" even though it is in fact a positively charged defect having more than one proton and water molecule involved in its definition (see ref 5 for more information). When the proton is far from the mouth of the nanotube, no significant change in the hydration can be observed. As the proton approaches the entrance (within a few Å), the number of pore water molecules increases from 2 to 4. As the proton enters the channel, it drags a few waters with it. Surprisingly though, once the proton has entered the mouth of the nanotube, the number of water molecules in the CNT *continues to increase* by having the waters *shuttle through* the excess proton charge defect. In other words, the proton "shoots" waters into the nanotube, thus creating its own "water wire" for subsequent transport. By the time the excess proton is 2−3 Å into the CNT, the tube transitions to the fully hydrated or "wet" state (Figure 1b).

To analyze the origin of water molecules that wet the CNT relative to the position of the excess proton, we traced the positions of the water oxygen atoms over the course of a simulation (Figure 1c). This demonstrates that water molecules originate on the same side of the graphene sheet as the excess proton defect and hence have to pass through it to enter the CNT. The length of the water wire ahead of the proton fluctuates until it connects with waters from the other side to fully wet the nanotube. Therefore, the transport of water molecules into the nanotube is enabled by an unusual manifestation of the Grotthuss shuttling mechanism involving the rearrangement of covalent bonds as water molecules *pass through* the relatively stationary protonic charge defect near the mouth of the channel.

To check whether other monatomic ions can also induce a similar wetting process, the same simulations were carried out with K^+ in place of an excess proton. Although K^+ pulls four water molecules into the nanotube, two on each flanking side, to form its hydration structure, it does not induce a full wetting transition (Figure 1d). The free energy profiles for the ion permeation (Figure 2a) are also different for H^+ and K^+. The energy barrier for K^+ to penetrate 5 Å into the CNT is over 30 kcal/mol, while that for the excess proton is less than 15 kcal/mol (see Figure 2a). The large difference in these two free energy profiles is consistent with the principal that the free energy barrier for an ion to enter a nanoconfined region is strongly influenced by the cost of dehydration. Since the excess proton can effectively keep part of its solvation shell as dynamical $H_5O_2^+$ and $H_7O_3^+$ structures,[27] it has a lower barrier for CNT penetration.

Moreover, the excess proton charge defect can transiently delocalize the net positive charge over even more water molecules and therefore reduce the dehydration penalty in this fashion. Similar to the situation with K^+, replacing the excess proton with a classical approximation of a hydronium cation (a simple ion with no possibility of Grotthuss shuttling and charge defect delocalization) also results in a large free energy cost for CNT penetration (>25 kcal/mol; see Figure 2a). Thus, the excess proton's ability to distribute the charge defect to surrounding water molecules within the CNT clearly also contributes to its decreased translocation barrier.

dx.doi.org/10.1021/jp5095118 | J. Phys. Chem. B 2015, 119, 9212−9218

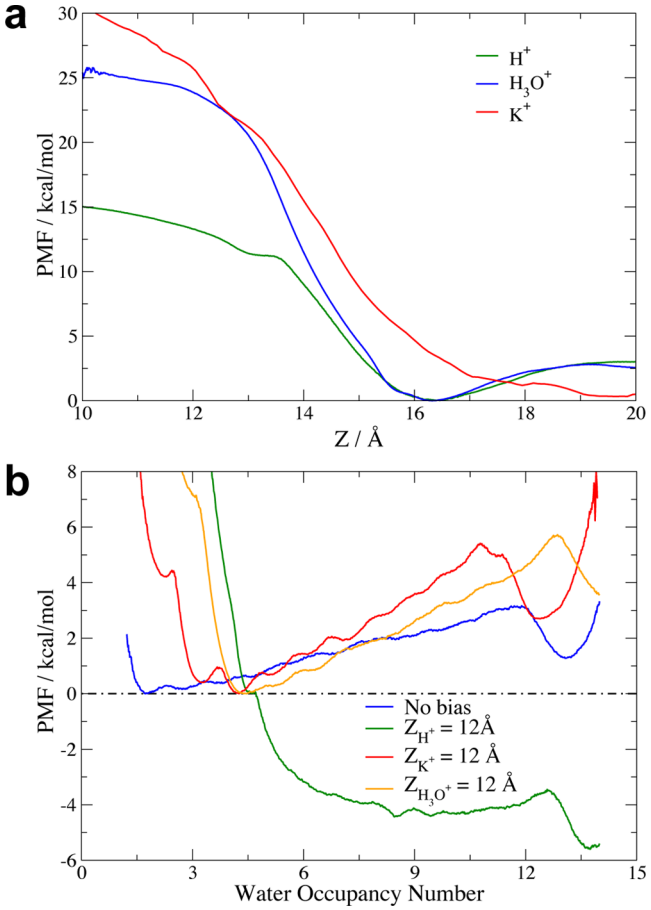

Figure 2. Free energy profiles of the ion permeation and the water occupancy in different simulation systems. (a) Free energy profiles from the permeations of different cations. The free energy of H^+ (the hydrated excess proton) has much lower energy barrier than the others, displaying the unique features of the excess H^+. (b) Free energy profiles of the water occupancy with the H^+ charge defect (green), K^+ (red), or classical H_3O^+ (yellow) fixed at Z = 12.0 Å (2−3 Å inside the mouth of the nanotube), compared to the result without the ions present (blue). The induced wetting process is only seen in the system with H^+. The average errors are (a) ±0.45 kcal/mol and (b) ±0.30 kcal/mol calculated from 500 ps block averages.

To further study the underlying mechanism of this proton induced CNT wetting process, a water occupancy reaction coordinate (see Methods, eqs 1−3) was defined to calculate the free energy profiles for nanotube wetting as well as those for ion transport at different hydration levels. First, we obtained the free energy profile of the wetting process in the absence of an ion (Figure 2b, blue curve). Similar to previous work,[21] the free energy profile of water occupancy has dry and wet minima (at N_w = 4 and N_w = 13, respectively) separated by a barrier (near N_w = 12). Consistent with a dry CNT, the fully wet (water occupied) state is ∼1 kcal/mol less stable than the dry state. However, when an excess proton is located in the region around Z = 12 Å (just 2−3 Å inside the CNT), the wetting free energy profile changes dramatically, as seen in Figure 2b, green curve. The wet minimum becomes ∼6 kcal/mol more stable such that wetting becomes spontaneous, and the transition along this wetting coordinate is nearly barrierless. This wetting behavior is not the case for the other ions, however. When a K^+ ion is located in the same location (Z = 12 Å), the barrier for wetting is increased to ∼5 kcal mol and the wet minima is destabilized by ∼2 kcal/mol (Figure 2b, red curve). The case for the classical H_3O^+ ion is even more dramatic, replacing the wet minimum with a 6 kcal/mol barrier (Figure 2b, yellow curve).

The collected results described above highlight the excess proton's unique ability to self-solvate and project outward a water wire into a hydrophobic space, thus wetting a dry region and thereby decreasing the barrier it has to overcome to transport through it. Such a phenomenon may have significant implications for understanding PT through hydrophobic regions of biomolecules and materials.

Coupled Mechanism for Proton Induced Wetting. The free energy profiles of Figure 2 indicate that the excess proton can induce the wetting of the hydrophobic nanotube and also that the proton has higher conductance (i.e., lower transport barrier) compared to K^+. Are the two processes related? To answer this, two independent collective variables, the water occupancy number and the position of the excess proton charge defect, were sampled from 325 simulation windows to construct a two-dimensional (2D) free energy surface. From the 2D surface (Figure 3), a fascinating coupled, stepwise

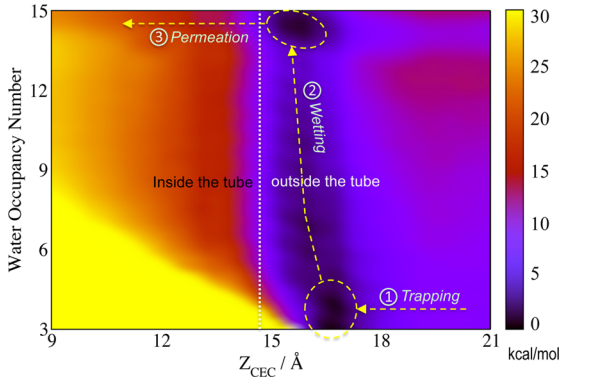

Figure 3. 2D free energy surface of the proton induced wetting process. The horizontal axis represents the Z-position of the hydrated excess proton charge defect, while the vertical axis represents the level of CNT water occupancy. The white dotted line (Z = 14.7 Å) indicates the position of the graphene layer and the mouth of the nanotube. A stepwise but coupled mechanism can be observed from the 2D free energy surface, in which three steps, trapping−wetting−permeation, are highlighted by yellow dashed arrows. The average errors are ±0.35 kcal/mol.

mechanism is clearly seen for the wetting and proton permeation. First, the excess proton is trapped close to the mouth of the nanotube in a free energy minimum ∼1 kcal/mol more stable than bulk. Hummer and collaborators have reported similar results with a proton minimum at the entry of the CNT.[26] This result is also consistent with the amphipathic nature of the hydrated proton, as reported in several theoretical studies.[52−54] The vacuum and nanotube wall are hydrophobic while bulk water and the graphene surface are more hydrophilic creating an amphipathic interface where the excess proton is stabilized. Second, after being trapped at the entry of the nanotube, the proton initiates the wetting transition described earlier by greatly lowering the free energy barrier for water penetration and stabilizing waters in the previously dry space (cf. Figure 2b). When the proton is ∼2−3 Å into the CNT (Z_{CEC} ≈ 12−13 Å in Figure 3), the relative free energy for wetting becomes very favorable with a negligible barrier (Figure 4a, blue, green, and red curves), transitioning

dx.doi.org/10.1021/jp5095118 | J. Phys. Chem. B 2015, 119, 9212−9218

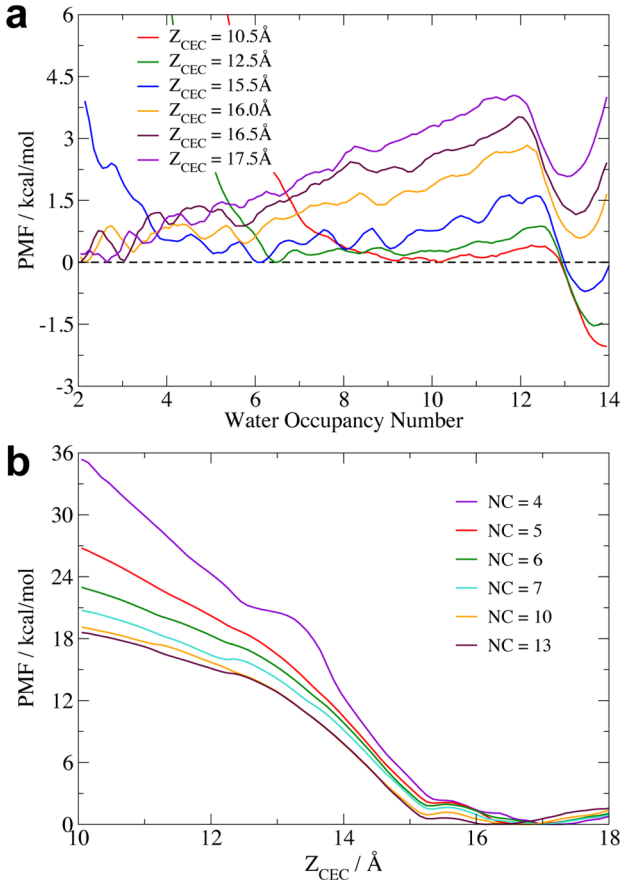

Figure 4. 1D free energy profiles extracted from the 2D free energy surface in Figure 3. (a) Free energy profiles of the wetting process when the excess proton charge defect is located at different positions along the nanotube axis. (b) Free energy profiles of proton permeation while the nanotube is in different hydration states where NC is defined as the number of confined waters in the nanotube. The average errors are ±0.35 kcal/mol.

the hydrophobic nanotube to the fully wet state. As the CNT hydration level increases, the barrier for the proton transport into the nanotube also greatly decreases (Figure 4b) and the proton can progress further into the CNT and eventually through via activated (barrier surmounting) dynamics. Indeed, the free energy penalty for the proton moving into the nanotube is greatly reduced from when the nanotube is dry. In fact, the free energy for proton permeation goes from >36 kcal/mol for the dry CNT, which is close to the energy barrier for K^+, to ∼18 kcal/mol for the fully wet CNT (Figure 4b). It is interesting to note that the lowest barrier for a constrained solvation state is 18 kcal/mol for NC = 13 (i.e., the fully wet state), while the free barrier with no solvation constraints is only 15 kcal/mol (Figure 2a). Thus, the proton induced wetting and proton permeation are dynamic and inherently coupled.

In summary, the 2D free energy surface in Figure 3 reveals the sensitivity of the CNT's solvation structure and stability to the position of the excess proton charge defect. The excess proton changes the water occupancy in the CNT even before it enters. Although the excess proton is weakly attracted to the entrance to the nanotube, it does not block water penetration as other ions will do. Instead *the excess proton defect shuttles waters through it* into the nanoconfined space via an unique manifestation of the Grotthuss shuttling mechanism, thereby lowering its own barrier for subsequent permeation.

Charge Delocalization Makes the Hydrated Excess Proton Unique. The 2D free energy surface for K^+ permeation versus nanotube hydration (Figure 5a) highlights

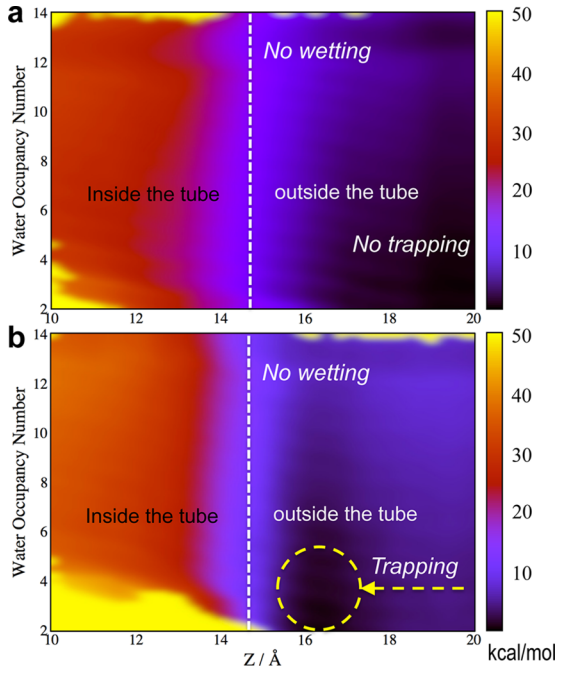

Figure 5. 2D free energy surfaces for (a) a K^+ cation and (b) a "classical" H_3O^+ (non-Grotthuss shuttling) cation showing the free energy for ion permeation relative to nanotube water occupancy and prepared in the same way as for Figure 3. The average errors are ±0.35 kcal/mol.

two important differences between H^+ and K^+. First, there is no energy minimum that indicates trapping at the mouth of the CNT. This is consistent with the common finding that K^+ prefers to be fully solvated in the bulk rather than at an interface. Second, there is no wetting profile. In fact, the wetting free energy shift (and barrier) remains positive no matter where the K^+ ion resides and is highest (least favorable) when K^+ is at the mouth of the CNT. Thus, K^+ blocks water entry whereas H^+ facilitates it. These contrasting effects are partially explained by the solvation dynamics. Consistent with previous studies, the water molecules in the CNT are highly mobile in the absence of ions, entering and leaving the tips of the nanotube frequently. However, when K^+ is near the entry of the nanotube, it blocks the water flux, which is entropically unfavorable. In contrast, water molecules in the presence of the excess proton charge defect at the entrance of the nanotube retain their ability to move in and out of the channel through the Grotthuss mechanism. Thus, delocalization of the excess proton charge defect is essential to decreasing the cost of wetting and ion permeation.

To confirm this hypothesis, we conducted another set of free energy surface calculations with a classical hydronium model (simple H_3O^+ cation), in which the charge defect delocalization and Grotthuss shuttling are disabled. As discussed above, the free energy profiles for H_3O^+ permeation and wetting (shown in Figure 2) are more similar to the results for K^+ than to those for H^+. The 2D free energy surface (Figure 5b) reveals that H_3O^+ also has a sort of trapping state near the mouth of the

dx.doi.org/10.1021/jp5095118 | J. Phys. Chem. B 2015, 119, 9212−9218

CNT as seen for H^+. However, the classical hydronium does not exhibit the favorable wetting transition (compare Figure 3 to Figure 5b). In fact, just as with K^+, water molecules are blocked from entering and leaving the CNT.

In order to quantify the degree of charge defect delocalization of the excess proton in the CNT, we analyzed the magnitude of excess positive charge owned by each water molecule in the simulations with H^+ restricted at Z = 12.5 Å. This is the case when the proton defect center of excess charge[2−4,24,37−40] coincides with the second CNT water molecule. When the nanotube is dry (N_w = 4), about 99% of the positive charge is distributed on three water molecules with the percentages 67%, 20%, and 12%, respectively. When the nanotube is fully wet (N_w = 14), the distribution shifts to 55%, 33%, and 10%. In the bulk,[2,5] the dominant species is the "distorted" Eigen cation, $H_9O_4^+$, with 62% of the charge on the central water molecule and the three surrounding waters that possess 19%, 10%, and 5% of the excess charge. The remaining 3−4% is on waters in the second solvation shell. Thus, although the charge defect delocalization in the CNT is weaker than it is in the bulk system, because of the strong spatial confinement, it is still significant. Moreover, it shifts to a more Zundel-like delocalized species in the fully wet nanotube,[27] which will contribute to the stabilization of the fully wet state. Thus, charge defect delocalization is again confirmed to be essential to the wetting mechanism and decreases the free energy barrier for ion permeation.

CONCLUDING REMARKS

For many years, studies of PT in biological systems have largely focused on the identification and the analysis of aqueous pathways interlaced with protonatable residues through which excess protons might migrate (especially via Grotthuss shuttling). Great effort has been devoted to characterizing internal hydration structures that connect protonatable residues to form such pathways. When hydrophobic cavities are encountered, i.e., those lacking crystallographically resolved water molecules, simulations have often been used to try to identify states of the system (e.g., via oxidation state or conformational changes) that induce wetting. In this manner, mechanisms of PT have been proposed based on the existence and stability of hydrogen-bonded water wires. However, the simulations presented herein suggest that the excess proton itself is strongly coupled to the solvation structure and stability in nanoconfined spaces and hence must be *explicitly included* in the analysis of internal solvation.

By simulating PT through a nanotube penetrating a graphene sheet with MS-RMD, we have discovered that a hydrated excess proton charge defect can induce wetting into a previously dry hydrophobic space. This is a novel wetting process in that water molecules actually *pass through the protonic charge defect via Grotthuss-like shuttling*. Other ions have the opposite effect, blocking the diffusion of water into the nanotube when they are close to the nanotube's entrance. Thus, this wetting process, which relies on charge defect delocalization and Grotthuss shuttling, is unique to a hydrated excess "proton" (though something similar may be possible for the hydroxide anion).

Although the present simulations have focused on PT through a CNT, our findings have broad implications for PT in biomolecular and materials systems. Just as our simulations have demonstrated in a CNT, an excess proton may actually transiently induce wetting in biomolecular hydrophobic cavities when it is located near a peripheral residue or water cluster. In this manner, the excess proton can create its own aqueous pathway for subsequent charge transport. As shown in this work, water rearrangement around a confined excess proton can be fast (from hundreds of picoseconds to several nanoseconds) relative to the rare events of biomolecular PT (typically microseconds or longer). Thus, with the strong correlation between solvation rearrangement and the position of a hydrated excess proton, the two processes of PT and wetting are likely to be strongly coupled (as demonstrated in the CNT). Indeed, the concept that PT requires an existing "water wire", e.g., one seen in an X-ray crystal structure or MD simulations without an explicit excess proton, should be questioned. What is more, computer simulations probing PT mechanisms should include an *explicit* treatment of the hydrated excess proton (along with its full physics of Grotthuss shuttling and charge defect delocalization) to properly capture the coupling between water dynamics, hydration, and PT. Using solvation structures to interpret PT mechanisms in the absence of an explicit excess proton can quite possibly lead to incorrect conclusions.

AUTHOR INFORMATION

Notes

The authors declare no competing financial interest.

ACKNOWLEDGMENTS

This research was supported by the National Institutes of Health (NIH Grant R01-GM053148) and the National Science Foundation (NSF Grant CHE-1214087). The authors acknowledge the University of Chicago Research Computing Center for computing resources and support. Computing facilities were also provided by the Extreme Science and Engineering Discovery Environment (XSEDE), which is supported by National Science Foundation Grant OCI-1053575.

REFERENCES

(1) Marx, D.; Tuckerman, M. E.; Hutter, J.; Parrinello, M. The Nature of the Hydrated Excess Proton in Water. *Nature* **1999**, *397*, 601−604.
(2) Schmitt, U. W.; Voth, G. A. The Computer Simulation of Proton Transport in Water. *J. Chem. Phys.* **1999**, *111*, 9361−9381.
(3) Wraight, C. A. Chance and Design—Proton Transfer in Water, Channels and Bioenergetic Proteins. *Biochim. Biophys. Acta, Bioenergetics* **2006**, *1757*, 886−912.
(4) Swanson, J. M. J.; Maupin, C. M.; Chen, H. N.; Petersen, M. K.; Xu, J. C.; Wu, Y. J.; Voth, G. A. Proton Solvation and Transport in Aqueous and Biomolecular Systems: Insights from Computer Simulations. *J. Phys. Chem. B* **2007**, *111*, 4300−4314.
(5) Knight, C.; Voth, G. A. The Curious Case of the Hydrated Proton. *Acc. Chem. Res.* **2012**, *45*, 101−109.
(6) Swanson, J. M. J.; Simons, J. Role of Charge Transfer in the Structure and Dynamics of the Hydrated Proton. *J. Phys. Chem. B* **2009**, *113*, 5149−5161.
(7) Markovitch, O.; Chen, H.; Izvekov, S.; Paesani, F.; Voth, G. A.; Agmon, N. Special Pair Dance and Partner Selection: Elementary Steps in Proton Transport in Liquid Water. *J. Phys. Chem. B* **2008**, *112*, 9456−9466.
(8) de Grotthuss, C. J. T. Sur la Décomposition de l'Eau et des Corps Qu'elle Tient en Dissolution à l'Aide de l'Électricité Galvanique. *Ann. Chim.* **1806**, *58*, 54−73.
(9) Agmon, N. The Grotthuss Mechanism. *Chem. Phys. Lett.* **1995**, *244*, 456−462.
(10) Kreuer, K. D. Proton Conductivity: Materials and Applications. *Chem. Mater.* **1996**, *8*, 610−641.

(11) Decoursey, T. E. Voltage-Gated Proton Channels and Other Proton Transfer Pathways. *Physiol. Rev.* **2003**, *83*, 475−579.
(12) Markovitch, O.; Agmon, N. Structure and Energetics of the Hydronium Hydration Shells. *J. Phys. Chem. A* **2007**, *111*, 2253−2256.
(13) Knight, C.; Lindberg, G. E.; Voth, G. A. Multiscale Reactive Molecular Dynamics. *J. Chem. Phys.* **2012**, *137*, 22A525.
(14) Garczarek, F.; Gerwert, K. Functional Waters in Intraprotein Proton Transfer Monitored by FTIR Difference Spectroscopy. *Nature* **2006**, *439*, 109−112.
(15) Henry, R. M.; Yu, C. H.; Rodinger, T.; Pomes, R. Functional Hydration and Conformational Gating of Proton Uptake in Cytochrome *c* Oxidase. *J. Mol. Biol.* **2009**, *387*, 1165−1185.
(16) Freier, E.; Wolf, S.; Gerwert, K. Proton Transfer via a Transient Linear Water-Molecule Chain in a Membrane Protein. *Proc. Natl. Acad. Sci. U.S.A.* **2011**, *108*, 11435−11439.
(17) Roux, B.; Nina, M.; Pomes, R.; Smith, J. C. Thermodynamic Stability of Water Molecules in the Bacteriorhodopsin Proton Channel: A Molecular Dynamics Free Energy Perturbation Study. *Biophys. J.* **1996**, *71*, 670−681.
(18) Otting, G.; Liepinsh, E.; Halle, B.; Frey, U. NMR Identification of Hydrophobic Cavities with Low Water Occupancies in Protein Structures Using Small Gas Molecules. *Nat. Struct. Biol.* **1997**, *4*, 396−404.
(19) Oprea, T. I.; Hummer, G.; Garcia, A. E. Identification of a Functional Water Channel in Cytochrome P450 Enzymes. *Proc. Natl. Acad. Sci. U.S.A.* **1997**, *94*, 2133−2138.
(20) Chakrabarty, S.; Warshel, A. Capturing the Energetics of Water Insertion in Biological Systems: The Water Flooding Approach. *Proteins* **2013**, *81*, 93−106.
(21) Hummer, G.; Rasaiah, J. C.; Noworyta, J. P. Water Conduction through the Hydrophobic Channel of a Carbon Nanotube. *Nature* **2001**, *414*, 188−190.
(22) Tao, Y. S.; Muramatsu, H.; Endo, M.; Kaneko, K. Evidence of Water Adsorption in Hydrophobic Nanospaces of Highly Pure Double-Walled Carbon Nanotubes. *J. Am. Chem. Soc.* **2010**, *132*, 1214−1215.
(23) Paineau, E.; Albouy, P. A.; Rouziere, S.; Orecchini, A.; Rols, S.; Launois, P. X-ray Scattering Determination of the Structure of Water During Carbon Nanotube Filling. *Nano Lett.* **2013**, *13*, 1751−1756.
(24) Brewer, M. L.; Schmitt, U. W.; Voth, G. A. The Formation and Dynamics of Proton Wires in Channel Environments. *Biophys. J.* **2001**, *80*, 1691−1702.
(25) Dellago, C.; Naor, M.; Hummer, G. Proton Transport through Water-Filled Carbon Nanotubes. *Phys. Rev. Lett.* **2003**, *90*, 105902.
(26) Dellago, C.; Hummer, G. Kinetics and Mechanism of Proton Transport across Membrane Nanopores. *Phys. Rev. Lett.* **2006**, *97*, 245901.
(27) Cao, Z.; Peng, Y. X.; Yan, T. Y.; Li, S.; Li, A. L.; Voth, G. A. Mechanism of Fast Proton Transport along One-Dimensional Water Chains Confined in Carbon Nanotubes. *J. Am. Chem. Soc.* **2010**, *132*, 11395−11397.
(28) Lee, S. H.; Rasaiah, J. C. Proton Transfer and the Diffusion of H^+ and OH^- Ions along Water Wires. *J. Chem. Phys.* **2013**, *139*, 124507.
(29) Lee, S. H.; Rasaiah, J. C. Note: Recombination of H^+ and OH^- Ions along Water Wires. *J. Chem. Phys.* **2013**, *139*, 36102.
(30) Choi, W.; Ulissi, Z. W.; Shimizu, S. F. E.; Bellisario, D. O.; Ellison, M. D.; Strano, M. S. Diameter-Dependent Ion Transport through the Interior of Isolated Single-Walled Carbon Nanotubes. *Nat. Commun.* **2013**, *4*, 2397.
(31) Wikström, M.; Verkhovsky, M. I.; Hummer, G. Water-Gated Mechanism of Proton Translocation by Cytochrome *c* Oxidase. *Biochim. Biophys. Acta, Bioenergetics* **2003**, *1604*, 61−65.
(32) Wang, D.; Voth, G. A. Proton Transport Pathway in the ClC Cl^-/H^+ Antiporter. *Biophys. J.* **2009**, *97*, 121−131.
(33) Han, W.; Cheng, R. C.; Maduke, M. C.; Tajkhorshid, E. Water Access Points and Hydration Pathways in ClC H^+/Cl^- Transporters. *Proc. Natl. Acad. Sci. U.S.A.* **2014**, *111*, 1819−1824.
(34) Zhu, F. Q.; Schulten, K. Water and Proton Conduction through Carbon Nanotubes as Models for Biological Channels. *Biophys. J.* **2003**, *85*, 236−244.
(35) Rasaiah, J. C.; Garde, S.; Hummer, G. Water in Nonpolar Confinement: From Nanotubes to Proteins and Beyond. *Annu. Rev. Phys. Chem.* **2008**, *59*, 713−740.
(36) Selvan, M. E.; Keffer, D. J.; Cui, S.; Paddison, S. J. Proton Transport in Water Confined in Carbon Nanotubes: A Reactive Molecular Dynamics Study. *Mol. Simul.* **2010**, *36*, 568−578.
(37) Kofinger, J.; Hummer, G.; Dellago, C. Single-File Water in Nanopores. *Phys. Chem. Chem. Phys.* **2011**, *13*, 15403−15417.
(38) Schmitt, U. W.; Voth, G. A. Multistate Empirical Valence Bond Model for Proton Transport in Water. *J. Phys. Chem. B* **1998**, *102*, 5547−5551.
(39) Day, T. J. F.; Soudackov, A. V.; Cuma, M.; Schmitt, U. W.; Voth, G. A. A Second Generation Multistate Empirical Valence Bond Model for Proton Transport in Aqueous Systems. *J. Chem. Phys.* **2002**, *117*, 5839−5849.
(40) Voth, G. A. Computer Simulation of Proton Solvation and Transport in Aqueous and Biomolecular Systems. *Acc. Chem. Res.* **2006**, *39*, 143−150.
(41) Wu, Y. J.; Chen, H. N.; Wang, F.; Paesani, F.; Voth, G. A. An Improved Multistate Empirical Valence Bond Model for Aqueous Proton Solvation and Transport. *J. Phys. Chem. B* **2008**, *112*, 467−482.
(42) Sumner, I.; Voth, G. A. Proton Transport Pathways in [NiFe]-Hydrogenase. *J. Phys. Chem. B* **2012**, *116*, 2917−2926.
(43) Savage, J.; Tse, Y. L. S.; Voth, G. A. Proton Transport Mechanism of Perfluorosulfonic Acid Membranes. *J. Phys. Chem. C* **2014**, *118*, 17436−17445.
(44) Liang, R. B.; Swanson, J. M. J.; Voth, G. A. Benchmark Study of the SCC-DFTB Approach for a Biomolecular Proton Channel. *J. Chem. Theory Comput.* **2014**, *10*, 451−462.
(45) Wu, Y. J.; Tepper, H. L.; Voth, G. A. Flexible Simple Point-Charge Water Model with Improved Liquid-State Properties. *J. Chem. Phys.* **2006**, *124*, 24503.
(46) MacKerell, A. D.; Bashford, D.; Bellott, M.; Dunbrack, R. L.; Evanseck, J. D.; Field, M. J.; Fischer, S.; Gao, J.; Guo, H.; Ha, S.; Joseph-McCarthy, D.; Kuchnir, L.; Kuczera, K.; Lau, F. T. K.; Mattos, C.; Michnick, S.; Ngo, T.; Nguyen, D. T.; Prodhom, B.; Reiher, W. E.; Roux, B.; Schlenkrich, M.; Smith, J. C.; Stote, R.; Straub, J.; Watanabe, M.; Wiorkiewicz-Kuczera, J.; Yin, D.; Karplus, M. All-Atom Empirical Potential for Molecular Modeling and Dynamics Studies of Proteins. *J. Phys. Chem. B* **1998**, *102*, 3586−3616.
(47) Yamashita, T.; Peng, Y. X.; Knight, C.; Voth, G. A. Computationally Efficient Multiconfigurational Reactive Molecular Dynamics. *J. Chem. Theory Comput.* **2012**, *8*, 4863−4875.
(48) Plimpton, S. Fast Parallel Algorithms for Short-Range Molecular-Dynamics. *J. Comput. Phys.* **1995**, *117*, 1−19.
(49) Deserno, M.; Holm, C. How To Mesh up Ewald Sums. II. An Accurate Error Estimate for the Particle-Particle-Particle-Mesh Algorithm. *J. Chem. Phys.* **1998**, *109*, 7694−7701.
(50) Kumar, S.; Bouzida, D.; Swendsen, R. H.; Kollman, P. A.; Rosenberg, J. M. The Weighted Histogram Analysis Method for Free-Energy Calculations on Biomolecules. 1. The Method. *J. Comput. Chem.* **1992**, *13*, 1011−1021.
(51) Liang, R.; Li, H.; Swanson, J. M.; Voth, G. A. Multiscale Simulation Reveals a Multifaceted Mechanism of Proton Permeation through the Influenza a M2 Proton Channel. *Proc. Natl. Acad. Sci. U.S.A.* **2014**, *111*, 9396−9401.
(52) Petersen, M. K.; Iyengar, S. S.; Day, T. J. F.; Voth, G. A. The Hydrated Proton at the Water Liquid/Vapor Interface. *J. Phys. Chem. B* **2004**, *108*, 14804−14806.
(53) Wang, F.; Izvekov, S.; Voth, G. A. Unusual "Amphiphilic" Association of Hydrated Protons in Strong Acid Solution. *J. Am. Chem. Soc.* **2008**, *130*, 3120−3126.
(54) Iuchi, S.; Chen, H. N.; Paesani, F.; Voth, G. A. Hydrated Excess Proton at Water−Hydrophobic Interfaces. *J. Phys. Chem. B* **2009**, *113*, 4017−4030.